Effects of Doping on the Vibrational Properties of C_{60} from First Principles: K_6C_{60}

Paolo Giannozzi[1,2] and Wanda Andreoni[2]
[1]*Scuola Normale Superiore and INFM, Piazza dei Cavalieri 7, I-56126 Pisa, Italy*
[2]*IBM Research Division, Zurich Research Laboratory, CH-8803 Rüschlikon, Switzerland*
(Received 13 November 1995; revised manuscript received 25 April 1996)

Ab initio calculations of the phonon spectrum of K_6C_{60} are presented, based on the local-density approximation of density-functional theory and on linear response theory. The effects of doping on frequencies and infrared intensities are identified and their physical origin discussed in detail for optically allowed modes. Whereas structural relaxation is primarily responsible for the frequency changes, and especially for the softening of tangential modes, the change in infrared relative intensities is a direct consequence of the electron transfer. The potassium vibrations are found to lie within $60-100\ \mathrm{cm}^{-1}$ and are well decoupled from C_{60} intramolecular modes. [S0031-9007(96)00397-3]

PACS numbers: 63.20.–e, 61.46.+w, 78.30.–j

Vital to progress in material science is the ability to control the changes induced in the electronic and mechanical properties of a reference material by doping it with foreign atoms. Raman and infrared (IR) spectra are the basic experimental tools adopted to inspect how doping modifies the structural and dynamical properties of the pristine material. A clear understanding of the physical origin of such changes is a prerequisite for making these spectra fingerprints, necessary to the design of new compounds.

Recently, solid C_{60} has become one of the most widely used reference materials. It is a ~ 1 eV gap semiconductor, which can be relatively easily tuned by metal intercalation, giving rise to a family of compounds called metal fullerides [1,2]. These are either semiconductors with different characteristics from C_{60} or metals or superconductors, depending on the concentration and the specific nature of the intercalating metal atoms. Well-resolved Raman and IR spectra are now available for a number of these compounds (see, e.g., [3–6]). They exhibit a highly mode-selective dependence both of the frequency shifts and the intensity variations, which suggests a complex electron-phonon interaction [7,8]. Basic questions are still open. For instance, in the case of the simplest intercalation, that with heavy alkali metals, the chemical picture is almost trivial, being electrons "fully" transferred to the molecular units. However, the modifications of the C_{60} phonon spectra is not trivial at all, and especially so their interpretation. One would like to at least be able to disentangle the mere effect of electron donation from that of the (consequent) structural relaxation of the molecule.

So far, trends with varying dopant concentration have been discussed mainly in terms of the charged phonon model [9]. This broadly associates the softening and enhancing of peaks with charge transfer and predicts a simple linear dependence of frequency shifts and a quadratic one of the IR intensities on the amount of charge transfer. The observed behavior is, however, much richer.

Going beyond this level of theory requires *ab initio* calculations of the phonon structure, which consistently treat electronic and structural variables. The attempts so far are a quantum-chemical calculation of the C_{60}^{6-} icosahedral I_h molecule [10], aimed at simulating $(K, Rb)_6C_{60}$ and a frozen-phonon calculation for K_3C_{60} [11] based on density functional theory in the local density approximation (DFT-LDA). The latter uses a minimal basis set and assumes a C_{60}. The results of I_h are only in fair agreement with experiment, and do not provide much insight into the microscopic mechanisms responsible for differences between the undoped and the doped materials. To this aim, we have performed an *ab initio* calculation of the phonon spectra of K_6C_{60} based on DFT-LDA and on the linear-response approach [12], and analyzed the results with a novel and convenient procedure.

The choice of K_6C_{60} [13] was motivated by three considerations: (i) Highly resolved single-crystal Raman and IR spectra have recently become available [4,5] that show a clear mode-selectivity of the doping-induced effects. (ii) The anomalies in its IR spectrum have been considered with special attention and recognized [7] as the signature of strong electron-phonon coupling. (iii) Our recent calculations of the structural and electronic properties of this system [14] are in good agreement with experiment.

Our results reproduce the experimentally observed changes in intensities and frequencies, and explain the different behavior of the various modes by isolating the various effects of the metal intercalation: the direct result of the electron transfer, and that of the changes in the molecular structure, as well as those due to intermolecular interaction in the solid. We also determine the vibrations of the cations, which lie at much lower frequencies and do not couple with the C_{60} intramolecular ones.

We follow the linear-response method, as previously applied to the vibrational and dielectric properties of the C_{60} molecule [15]. The technical details are the same as in [15]. We use norm-conserving LDA pseudopotentials to represent the electron-ion interaction, and a plane-wave basis set. For potassium we use a one-electron pseudopotential (1e-nlcc) [14], which incorporates the nonlinear core correction of the exchange and correlation functionals, needed to account for the effects of the core-valence

TABLE I. Calculated vibrational frequencies of C_{60}-like modes in K_6C_{60}. Bold: Optically active modes. Units are cm^{-1}.

A_g		474	**507**	562	692	1137	1352	**1469**	1492
A_u	323	711	743	926	941	1345	1451		
E_g		**266**	**419**	**660**	**769**	**1109**	**1268**	**1414**	**1498**
E_u	378	478	627	678	1161	1328	1462		
T_g			**274**	**412**	461	526	537	560	**660**
	666	740	**770**	792	808	**1107**	1140	**1264**	1298
	1340	1360	**1423**	1487	**1508**				
T_u				342	363	377	**466**	488	**571**
	626	666	668	706	744	949	1018	1172	**1215**
	1240	1332	1350	**1395**	1453	1461	1476		

overlap. The same approach was used to calculate [14] the structural and bonding properties of K_6C_{60} [16]. This is a semiconductor with an energy gap of $\approx$0.8 eV between the t_{1u}- and t_{1g}-derived C_{60} states [17]. The chemical bonding is strongly ionic with an almost complete charge transfer to C_{60}. The main change induced in the molecular conformation is the lengthening of the double bonds, especially those along the crystal axis. Solid-state effects, namely finite volume and symmetry lowering, are weak but detectable in the distribution of the electron density as measured in nuclear magnetic resonance experiments [18]. The vibrational properties are expected to be more sensitive than the electronic ones to distortions in the molecular structure.

In Table I, we list the spectrum of the zone-center C_{60} phonons with the labeling of the cubic symmetry group [3]. A global softening of the molecular spectrum results, and the symmetry lowering splits the vibrational modes of the I_h molecule [3]. We shall focus on the optically allowed phonons (A_g, E_g, and T_g are the Raman active, T_u the IR) and especially those derived from the modes which are optically allowed for the C_{60} molecule (A_g, H_g are the Raman active, T_{1u} the IR). Table II compares theory and experiment. The agreement with experiment is within 3%, and apart from the one case [$H_g(5)$], the shifts with respect to C_{60} are well reproduced.

In order to establish the origin of these changes, we have calculated the vibrational spectra of the following ideal systems: (I) a bcc C_{60} at the volume of K_6C_{60} with the molecules kept in the molecular I_h structure, (II) a bcc C_{60} with the molecules deformed as in K_6C_{60}, and (III) K_6C_{60} with the molecule kept in the molecular I_h structure. Comparing the C_{60} molecule with (I) allows us to determine the effects of the solid; (I) with (II) elucidates those of the molecular deformation by itself; (III) with (I) isolates the direct influence of the charge transfer. Finally, contrasting the real K_6C_{60} (IV) with (III) establishes the effects of the molecular relaxation in the presence of the excess electrons.

Figure 1 summarizes all this information for each of the optically active C_{60}-like modes by plotting the frequency shifts for systems (I) through (IV) with respect to C_{60}. The final change is seldom dominated by only one mechanism. Both direct charge transfer and structural relaxation affect each mode in a different way, may harden or soften them, or even leave them unaffected. Solid-state effects are very weak. Let us discuss some specific examples. As experimentally measured, the $A_g(1)$ breathing mode is only slightly affected by doping (also in agreement with the small change of the molecular radius) [19], whereas the "pinch" $A_g(2)$ mode largely softens ($\Delta\omega = -35$ cm^{-1}). This redshift increases almost linearly with increasing concentration of the dopant and is used as a measure either of the charge transfer or of the concentration itself. However, the mere electron transfer would increase its frequency (by 26 cm^{-1} in K_6C_{60}). It is the structural relaxation which decreases it and dominates. This is the mechanism which is primarily responsible for the softening of the other modes as well, especially the IR $T_{1u}(4)$ and

TABLE II. K_6C_{60}: Theoretical and experimental frequencies ω of the optically C_{60}-like active modes and shifts $\Delta\omega$ with respect to C_{60}. We use the labeling of the I_h group. The H_g modes split into a triplet T_g (left) and a doublet E_g (right). The experimental values are ascribed according to the calculated ordering. Their shifts refer to the centers of gravity. Units are cm^{-1}.

	ω			$\Delta\omega$	
Mode	Theory	Exp. [3]	Exp. [6]	Theory	Exp. [3,6]
$A_g(1)$	507	502	501	12	9, 6
$A_g(2)$	1469	1432	1431	−35	−36, −36
$H_g(1)$	274, 266	281, 269	280, 268	11	6, 5
$H_g(2)$	412, 419	419, 427	419, 427	−12	−8, −9
$H_g(3)$	660, 660	656, 676	656, 676	−51	−44, −47
$H_g(4)$	770, 769	761	760, 728	−13	−11, −25
$H_g(5)$	1107, 1109	1094, 1120	1093, 1122	−12	5, 6
$H_g(6)$	1264, 1268	1237	1232, 1237	−15	−11, −14
$H_g(7)$	1423, 1414	1383	1384	−31	−43, −38
$H_g(8)$	1508, 1498	1476	1481, 1474	−74	−97, −95
		Exp. [4]	Exp. [5]		Exp. [4,5]
$T_{1u}(1)$	466	467	467	−61	−61, −60
$T_{1u}(2)$	571	565	564	−15	−12, −12
$T_{1u}(3)$	1215	1182	1183	−3	0, 0
$T_{1u}(4)$	1395	1340	1341	−67	−86, −88

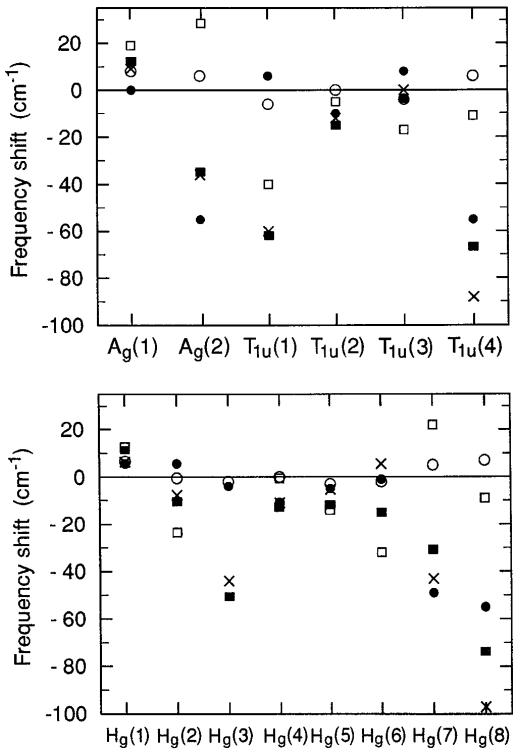

FIG. 1. K_6C_{60} frequency shifts (in cm^{-1}) of the optically active C_{60}-like modes. Filled squares: the real system (IV). Empty circles: system I. Filled circles: system II. Empty squares: system III (see text). Crosses: experiment. (From Refs. [5] and [3] for IR and Raman active modes, respectively.)

the Raman active $H_g(7)$, and $H_g(8)$. The picture is not as simple, however. There are cases, such as the $H_g(2)$ and $T_{1u}(3)$ for which structural changes tend to harden slightly. Also, for $H_g(3)$, the redshift is large ($\Delta\omega = -50\ cm^{-1}$) but is exclusively due to the electron transfer.

A strong mode dependence of the frequency shifts was also found for the $Li_{12}C_{60}$ molecule [20], and the role of the double-bond lengthening in causing a significant softening of tangential modes was pointed out.

The IR spectrum of K_6C_{60} is interesting in view not only of the doping-induced frequency shifts (see Table I), but also of the intensity changes (see Table III). These features have long been regarded as signatures of a mode-selective electron-phonon coupling [7], but a satisfactory interpretation is still lacking. Reference [12] has provided a general method for the calculation of IR oscillator strengths from linear-response DFT. In [15], this was successfully applied to C_{60}. The oscillator strength of the νth mode is given by

TABLE III. Calculated intensity enhancement of the IR-active T_{1u} modes (see text) and comparison with experimental data.

Label	Theory	Ref. [5]	Ref. [4]	Ref. [7]
$T_{1u}(1)$	3	2	1.5	2
$T_{1u}(2)$	35	21	21	33
$T_{1u}(3)$	8	2.5	6	3
$T_{1u}(4)$	150	83	80	88

$$f(\nu) = \sum_{\alpha} \left| \sum_{i\beta} Z^{\star}_{\alpha\beta}(i) e_{\beta}(i|\nu) \right|^2, \tag{1}$$

where $e_\beta(i|\nu)$ is the normalized eigenmode, α and β are Cartesian polarizations, i runs over the atoms in the unit cell, and $Z^{\star}_{\alpha\beta}(i)$ is the effective-charge tensor [12]

$$Z^{*}_{\alpha\beta}(i) = Z_v(i)\delta_{\alpha\beta} + \frac{4}{N} \sum_{\mathbf{k}\in \mathrm{BZ}} \sum_{v} \sum_{c} \times \frac{\langle \psi_{v,\mathbf{k}} | \delta V^{\mathrm{ph,bare}}_{\beta}(i) | \psi_{c,\mathbf{k}} \rangle \langle \psi_{c,\mathbf{k}} | \delta V^{E,\mathrm{scf}}_{\alpha} | \psi_{v,\mathbf{k}} \rangle}{\epsilon_{c,\mathbf{k}} - \epsilon_{v,\mathbf{k}}}. \tag{2}$$

Z_v is the ionic charge, BZ stands for the Brillouin zone, $\epsilon_{v,\mathbf{k}}$ and $\epsilon_{c,\mathbf{k}}$ denote valence and conduction bands, respectively, $\psi_{v,\mathbf{k}}$ and $\psi_{c,\mathbf{k}}$ the Kohn-Sham states, $\delta V^{\mathrm{ph,bare}}_{\beta}(i)$ the linear variation of the bare electron ion potential with respect to a displacement of the ith atom along the β direction, and $\delta V^{E,\mathrm{scf}}_{\alpha}$ that of the screened potential with respect to an applied electric field.

We reduce the sum over the BZ to the P point [17] as for the electron density [14]. The k summation in Eq. (2) is more slowly convergent, so the calculated intensities must be considered only an estimate. Of central interest here is their change from C_{60} to K_6C_{60}, rather than their absolute values. To minimize the convergence error, we consider also C_{60} in a bcc solid, and evaluate the intensities for the two systems with the same atomic density (our system I) within the same approximation. The intensity ratios, Table III, are compared with the values from experiment.

In agreement with experimental observation: (i) All the IR intensities are enhanced as a result of doping—a fact readily understandable as a consequence of the decrease of the effective energy gaps $\epsilon_{v,\mathbf{k}}$-$\epsilon_{c,\mathbf{k}}$ in Eq. (2). This is reflected in the dielectric constant ϵ_0, for which we calculate an increase by $\sim$3 from bulk C_{60} ($\epsilon_0 = 4.4$) to K_6C_{60} ($\epsilon_0 = 12.2$). (ii) An important change in the relative intensities of the four T_{1u} modes takes place, and $T_{1u}(2)$ and $T_{1u}(4)$ become prominent.

Our analysis in terms of the I-IV systems shows that the variation of the IR intensities and of the dielectric constant is dominated by the direct effect of the electron transfer. In fact, the values obtained for our system (III) are almost identical with the final ones. The structural relaxation has only a minor influence. This is at odds with the phonon frequency changes, for which it plays the major role, and explains in particular why the softening of an IR active mode is not necessarily accompanied by an enhancement of its intensity. In fact, a modest IR intensity is observed for $T_{1u}(1)$ in spite of the measured large frequency change, and vice versa for $T_{1u}(2)$. In the case of $T_{1u}(4)$, for which both frequency and intensity change in a dramatic way, the dominant mechanisms are also different, the former being due to the structural relaxation [see Fig. 1(a)].

So far, the interpretation of the IR spectrum has relied on the charged phonon model, which neglects structural

TABLE IV. Calculated vibrational frequencies of potassium ions in K_6C_{60}. The two lines refer to two different calculations as explained in the text. Units are cm^{-1}.

K-pseudo	A_g	E_g	T_g	T_u
1e-nlcc	68	102	83; 123	82; 95; 129
9e	64	98	60; 97	63; 89; 99

relaxation. As a consequence of the charge transfer only, it predicts the occurrence of a simultaneous softening and intensity enhancement for any mode that couples the t_{1u} to the t_{1g} orbitals. This could qualitatively account for the observed behavior of $T_{1u}(2)$ and $T_{1u}(4)$. However, in view of the above discussion, this picture is oversimplified. We have also analyzed the validity of a two-level (t_{1u}-t_{1g}) model for calculating the IR intensity, by extracting the contribution of the individual electronic excitations to the effective charges in Eq. (2). The situation is much more complex, and only in the case of $T_{1u}(4)$ can the t_{1u}-t_{1g} channel be considered the dominant one [21].

In Table IV, we list the frequencies of the vibrational modes of K, which turn out to be decoupled from the rest. Raman spectra [22] exhibit a relatively intense peak at 33 cm^{-1}, a weak shoulder at 48 cm^{-1}, a broad band at $\sim$ 75 cm^{-1}, and a peak with resonant character at 105 cm^{-1}. The lowest one was ascribed to the librational mode of C_{60}, and the rest to the cations. The K atoms at equilibrium occupy quasitetrahedral sites $(0.25-\delta, 0, 0.5)$ on the faces of the cube. Their Raman active modes are four: one A_g, which can be described as the breathing of the rhombohedral cluster, one E_g, and two T_g. Only the E_g doublet could be experimentally assigned, at 105 cm^{-1}, on the basis of its resonance properties. Our calculations performed with the 1e-nlcc pseudopotential (first row in Table IV) yield the E_g doublet at 102 cm^{-1}, but do not predict any Raman intensity below 68 cm^{-1}. To check the accuracy of these results, we have performed the entire phonon calculation again, using a 9e-pseudopotential which reduces the frozen core to the $n = 1$ and $n = 2$ shells [23]. In this way, the $3s$ and $3p$ electrons can relax in response to the ionization of the metal atom. As expected, the newly optimized structure for the molecule and also the intramolecular spectrum are unchanged. The change of the K positions is limited (δ varies from 0.026 to 0.021), but some of the Raman modes are sensitive to the core polarization, which lowers their frequencies significantly. Still the active range seems to be somewhat narrower than the observed one. We cannot exclude further softening due to anharmonicity. However, a confirmation of the Raman response and also far-IR measurements are desirable for a better evaluation of our results.

In conclusion, we have shown that the linear-response DFT-LDA approach combined with a full structural relaxation is able to describe accurately the doping-induced effects on the vibrational spectrum of a solid fulleride and account for the observed mode selectivity. A general framework is also provided to identify the underlying physical mechanisms responsible for changes both in frequencies and in intensities. It may be seen as a guide for the description of the electron-phonon interaction in these materials and also for the interpretation of other metal-C_{60}-based systems (see, e.g., [24]).

We are grateful to R. L. Whetten, M. J. Rice, E. Tosatti, F. Zerbetto, C. Taliani, H. Kuzmany, and M. Meneghetti for useful discussions and P. Guéret for useful comments on the manuscript.

[1] R. C. Haddon, Acc. Chem. Res. **25**, 127 (1992).
[2] J. E. Fischer *et al.*, J. Phys. Chem. Solids **56**, 1445 (1995), and references therein.
[3] P. C. Eklund *et al.*, J. Phys. Chem. Solids **53**, 1391 (1992).
[4] M. C. Martin, D. Koller, and L. Mihaly, Phys. Rev. B **47**, 14 607 (1993).
[5] T. Pichler, R. Winkler, and H. Kuzmany, Phys. Rev. B **49**, 15 879 (1994).
[6] H. Kuzmany *et al.*, Adv. Mater. **6**, 731 (1994).
[7] K.-J. Fu *et al.*, Phys. Rev. B **46**, 1937 (1992).
[8] V. P. Antropov, O. Gunnarsson, and A. I. Lichtenstein, Phys. Rev. B **48**, 7651 (1993); O. Gunnarsson *et al.*, Phys. Rev. Lett. **74**, 1875 (1995).
[9] M. J. Rice and H. Y. Choi, Phys. Rev. B **45**, 10 173 (1992).
[10] F. Negri, G. Orlandi, and F. Zerbetto, Chem. Phys. Lett. **196**, 303 (1992).
[11] K.-P. Bohnen *et al.*, Phys. Rev. B **51**, 5805 (1995).
[12] S. Baroni, P. Giannozzi, and A. Testa, Phys. Rev. Lett. **58**, 1861 (1987); P. Giannozzi *et al.*, Phys. Rev. B **43**, 7231 (1991).
[13] O. Zhou *et al.*, Nature (London) **351**, 6326 (1991).
[14] W. Andreoni, P. Giannozzi, and M. Parrinello, Phys. Rev. B **51**, 2087 (1995).
[15] P. Giannozzi and S. Baroni, J. Chem. Phys. **100**, 8537 (1994).
[16] In Ref. [14] an energy cutoff of 35 Ryd was used for the plane wave expansion of the electron wave function. Here we use a higher cutoff (45 Ryd) to have a better description of the dynamical properties. Negligible differences (<0.003 Å) result in the equilibrium bond lengths.
[17] The absence of an energy gap, as in the case of K_3C_{60}, renders accurate calculations much more demanding.
[18] F. Rachdi *et al.*, Solid State Commun. **87**, 547 (1993).
[19] R. A. Jishi and M. S. Dresselhaus, Phys. Rev. B **45**, 6914 (1992).
[20] J. Kohanoff, W. Andreoni, and M. Parrinello, Chem. Phys. Lett. **198**, 472 (1992).
[21] The t_{1u}-t_{1g} channel is absent in C_{60}. The valence electrons states are in h_u orbitals, whose first dipole-allowed coupling is to the t_{1g} separated by more than 2 eV.
[22] V. N. Denisov *et al.*, Synth. Met. **64**, 341 (1994).
[23] Calculations with both pseudopotentials reproduce the experimental values for the interatomic distance of K_2 within 1% and that of the vibrational frequency within 5%.
[24] S. Modesti, S. Cerasari, and P. Rudolf, Phys. Rev. Lett. **71**, 2469 (1993).